Int. J. Solids Structures Vol. 26, No. 9/10, pp. 1143–1157, 1990
Printed in Great Britain.

0020–7683/90 $3.00 + .00

AN ANALYTIC–ASYMPTOTIC APPROACH FOR TIME-HARMONIC NONSYMMETRIC WAVE PROPAGATION IN A CYLINDER

YOON YOUNG KIM and CHARLES R. STEELE
Division of Applied Mechanics, Durand Building, Stanford University, Stanford, CA 94305, U.S.A.

Abstract—A solution approach for general nonsymmetric time-harmonic end problems is demonstrated for a semi-infinite isotropic solid circular cylinder which is traction-free on its cylindrical surface. The present solution technique is an extension of that used in Kim and Steele (1989a, *J. Appl. Mech.* **56**, 334–346) for longitudinal axisymmetric wave propagation in a cylinder. In the present solution procedure, the end displacement and traction are expanded by the series found by Kim and Steele (1989b, *J. Appl. Mech.* **56**, 910–917), and the end stiffness matrix is formed. The insensitive nature of the solutions at the end of the cylinder to cylindrical surface conditions, as observed by Kim and Steele (1989b), is utilized in the present solution procedure. The effectiveness of the approach is demonstrated by an example of localized eccentric loading of the end.

1. INTRODUCTION

There has been a revived interest in the problem of elastic wave propagation in cylinders in recent years.† Nondestructive evaluation and accurate dynamic modeling of some high-precision instruments may be the thrust for such a trend. However, it appears that an accurate, yet efficient solution technique is still not available for solving general end problems. Obviously, such a solution technique must be valid for both axisymmetric and nonsymmetric wave propagation.

Devault and Curtis (1962) studied a mixed time-dependent end condition for which either the normal stress and tangential displacements or the normal displacement and the tangential stresses are specified at the end. Wilson (1986) used the results obtained by McKenna and Simpkins (1985) to solve a mixed end problem. Very recently Shen (1988) used the modal expansion in order to study transient waves by a normal point force applied on the cylindrical surface. None of these investigators has considered the pure end conditions for which either the three stress components or the three displacement components are specified at the end. Instead, they approximate the pure end conditions by means of the mixed conditions, which results in mathematical simplicity. Though assuming the mixed end conditions for the pure end conditions may be reasonable for far-field solutions, it appears that there is a need to handle the pure end conditions for either near-field or more accurate far-field solutions.

The existing solution techniques based on the elasticity solutions such as collocation (see, e.g. Zemanek, 1972) may be used for the general nonsymmetric case. However, the numerical difficulties for the nonsymmetric case become more severe than for the axisymmetric case because more displacements and/or stresses need to be matched at the end of the cylinder.

In the present work, a solution technique is proposed as an effective alternative to conventional solution approaches such as collocation and finite elements for the analysis of time-harmonic nonsymmetric wave propagation in an isotropic semi-infinite solid cylinder, which is traction-free on its cylindrical surface. The present approach is an extension of the solution technique proposed by Kim and Steele (1989a) for the axisymmetric case to the general nonsymmetric case. Kim and Steele (1989a) use the end stiffness matrix which relates the harmonics of the displacements and stresses at the end of the cylinder. The expansion sets are the series solutions of an uncoupled wave system, which yields a stiffness matrix of a form which can be utilized for an efficient solution technique.

† The history of the analysis of the elastic waves is well described in review papers by Green (1960), Miklowitz (1966), McNiven and McCoy (1974) and Pao (1983).

Unlike the solution approach proposed by Kim and Steele (1989a) for the axisymmetric case, the present approach for the nonsymmetric case uses the end stiffness matrix that relates the normal components of the displacement and stress and the modified displacement and stress quantities which Kim and Steele (1989b) have introduced. The end stiffness matrix does not simply relate the usual displacement and stress quantities. The use of such a stiffness matrix is crucial; first, closed-form expressions are possible for the elements of the stiffness matrix. Furthermore, the present stiffness matrix for the traction-free case also exhibits some asymptotic behavior, which can be utilized to enhance numerical efficiency.

For the nonsymmetric case, the proper expansions are provided by the new series solutions by Kim and Steele (1989b) corresponding to an uncoupled wave system in a cylinder which has been found by Kim (1989a). The stiffness matrix based on the expansions is shown to be asymptotically equivalent to the stiffness matrix for the uncoupled wave system, for which the harmonics are decoupled. The consequence of the asymptotic behavior is that the stiffness matrix can be partitioned into a coupled system for lower harmonics and a weakly coupled system for higher harmonics. Therefore, even very rapidly varying end conditions which require a large number of harmonics can be handled effectively.

The asymptotic behavior is examined numerically, and the present stiffness matrix approach is applied to some numerical examples and compared with the collocation method. The reduction in the CPU time by the present method appears to be substantial even without incorporating the asymptotic behavior of the stiffness matrix.

2. PRELIMINARIES

A solution to the wave equation for an isotropic elastic solid cylinder can be expressed (see Kim, 1989a for detailed expressions and notations) as

$$\mathbf{u}(r,\theta,z,t) = \tilde{\mathbf{u}}(r)\begin{Bmatrix}\cos n\theta\\ \sin n\theta\end{Bmatrix}\exp\left[\mathrm{i}(\lambda z-\Omega t)\right]$$

$$\boldsymbol{\sigma}(r,\theta,z,t) = \tilde{\boldsymbol{\sigma}}(r)\begin{Bmatrix}\cos n\theta\\ \sin n\theta\end{Bmatrix}\exp\left[\mathrm{i}(\lambda z-\Omega t)\right] \tag{1}$$

where

$$\tilde{u}_r(r) = A\frac{\mathrm{d}J_n(hr)}{\mathrm{d}r} + B(\mathrm{i}\lambda)\frac{\mathrm{d}J_n(kr)}{\mathrm{d}r} - C\frac{n}{r}J_n(kr) \tag{2a}$$

$$\tilde{u}_\theta(r) = -A\frac{n}{r}J_n(hr) - B(\mathrm{i}\lambda)\frac{n}{r}J_n(kr) + C\frac{\mathrm{d}J_n(kr)}{\mathrm{d}r} \tag{2b}$$

$$\tilde{u}_z(r) = A(\mathrm{i}\lambda)J_n(hr) + Bk^2J_n(kr). \tag{2c}$$

Displacement $\mathbf{u}$ and stress $\boldsymbol{\sigma}$ are the physical quantities divided by a, the radius of cylinder, and 2μ, twice the shear modulus, respectively. The ratios of the radial and axial coordinates to a are denoted by r and z. The dimensionless wave number λ is defined as $2\pi a/L$ where L is the wavelength. We also define the dimensionless frequency Ω and t as $\omega a/c_s$ and $\tau c_s/a$ where ω is the angular frequency, c_s is the shear wave speed, and τ is the time. The parameters h^2 and k^2 are defined as

$$h^2 = \alpha^2\Omega^2 - \lambda^2; \quad k^2 = \Omega^2 - \lambda^2.$$

The material property α^2 is related to Poisson's ratio ν:

$$\alpha^2 = \frac{1-2\nu}{2(1-\nu)}.$$

In (1), u_θ, $\sigma_{r\theta}$, and $\sigma_{\theta z}$ take sin $n\theta$, and the other quantities take cos $n\theta$.

For a cylinder with a traction-free cylindrical surface (which will be called the traction-free cylinder from now on), the frequency equation results in complicated dispersion relations (see, e.g. Kim, 1989a; Shen, 1988) and the solutions for general end conditions are difficult to obtain. Due to the bi-orthogonality condition (Frazer, 1975; Gregory, 1983), however, solutions for mixed end conditions can be easily obtained. If the general solution form for the traction-free cylinder is written for a given frequency Ω as

$$\begin{Bmatrix} \mathbf{u}(r,\theta,z,t) \\ \boldsymbol{\sigma}(r,\theta,z,t) \end{Bmatrix} = \sum_{p=1}^{\infty} E^p \begin{Bmatrix} \tilde{\mathbf{u}}^p(r) \\ \tilde{\boldsymbol{\sigma}}^p(r) \end{Bmatrix} \begin{Bmatrix} \cos n\theta \\ \sin n\theta \end{Bmatrix} \exp[\mathrm{i}(\lambda^p z - \Omega t)], \tag{3}$$

where the pth expansion coefficient E^p can be easily determined for mixed end conditions,

$$E^p = \left\{ \begin{array}{c} \displaystyle\int_0^1 [\tilde{\sigma}^p_{zz}(r)U_z(r) - \tilde{u}^p_r(r)S_r(r) - \tilde{u}^p_\theta(r)S_\theta(r)]\, r\, \mathrm{d}r \\ \hline \displaystyle\int_0^1 [\tilde{\sigma}^p_{zz}(r)\tilde{u}^p_z(r) - \tilde{u}^p_r(r)\tilde{\sigma}^p_{rz}(r) - \tilde{u}^p_\theta(r)\tilde{\sigma}^p_{\theta z}(r)]\, r\, \mathrm{d}r \\ \displaystyle\int_0^1 [\tilde{u}^p_z(r)S_z(r) - \tilde{\sigma}^p_{rz}(r)U_r(r) - \tilde{\sigma}^p_{r\theta}(r)U_\theta(r)]\, r\, \mathrm{d}r \\ \hline \displaystyle\int_0^1 [\tilde{\sigma}^p_{zz}(r)\tilde{u}^p_z(r) - \tilde{u}^p_r(r)\tilde{\sigma}^p_{rz}(r) - \tilde{u}^p_\theta(r)\tilde{\sigma}^p_{\theta z}(r)]\, r\, \mathrm{d}r \end{array} \right\} \equiv \frac{N^p}{D^p} \tag{4}$$

with the notation†

$$U_r(r) = u_r|_{z=0}; \quad U_\theta(r) = u_\theta|_{z=0}; \quad U_z(r) = u_z|_{z=0};$$
$$S_r(r) = \sigma_{rz}|_{z=0}; \quad S_\theta(r) = \sigma_{r\theta}|_{z=0}; \quad S_z(r) = \sigma_{zz}|_{z=0}.$$

It is possible (Kim, 1989a) to have an uncoupled wave system corresponding to the following condition on the cylindrical surface:

$$u_r = 0; \quad \sigma_{rz} = 0; \quad \sigma_{r\theta} + u_\theta = 0. \tag{5}$$

The latter condition corresponds to a distributed spring restraint in the circumferential direction. Kim and Steele (1989b) show that the solutions of the cylinder with the condition (5) provide new series which can be written as

$$U_r(r) = \sum_{m=1}^{\infty} \left[-\frac{U_m}{\xi_m} \frac{\mathrm{d}J_n(\xi_m r)}{\mathrm{d}r} + \frac{V_m}{\rho_m} \frac{n}{r} J_n(\rho_m r) \right] \tag{6a}$$

$$U_\theta(r) = \sum_{m=1}^{\infty} \left[\frac{U_m}{\xi_m} \frac{n}{r} J_n(\xi_m r) - \frac{V_m}{\rho_m} \frac{\mathrm{d}J_n(\rho_m r)}{\mathrm{d}r} \right] \tag{6b}$$

$$U_z(r) = \sum_{m=1}^{\infty} W_m J_n(\xi_m r) \tag{6c}$$

and

$$S_r(r) = \sum_{m=1}^{\infty} \left[-\frac{S_m}{\xi_m} \frac{\mathrm{d}J_n(\xi_m r)}{\mathrm{d}r} + \frac{T_m}{\rho_m} \frac{n}{r} J_n(\rho_m r) \right] \tag{7a}$$

$$S_\theta(r) = \sum_{m=1}^{\infty} \left[\frac{S_m}{\xi_m} \frac{n}{r} J_n(\xi_m r) - \frac{T_m}{\rho_m} \frac{\mathrm{d}J_n(\rho_m r)}{\mathrm{d}r} \right] \tag{7b}$$

† The dependence of the displacement and stress on t and θ will be omitted.

$$S_z(r) = \sum_{m=1}^{\infty} Z_m J_n(\xi_m r) \tag{7c}$$

where ξ and ρ are the solutions of $J_n'(\xi) = 0$ and $J_n(\rho) = 0$, respectively. The explicit expressions for the expansion coefficients U_m, V_m, W_m, etc. are given in Kim and Steele (1989b). The formulas for calculation of these coefficients are uncoupled.

The expansions (6) and (7) for the displacement and stress at the end of the cylinder are equivalent to (Kim and Steele, 1989b)

$$U_I(r) = \sum_{m=1}^{\infty} U_m \xi_m J_n(\xi_m r) \tag{8a}$$

$$U_{II}(r) = \sum_{m=1}^{\infty} V_m \rho_m J_n(\rho_m r) \tag{8b}$$

$$U_z(r) = \sum_{m=1}^{\infty} W_m J_n(\xi_m r) \tag{8c}$$

$$S_I(r) = \sum_{m=1}^{\infty} S_m \xi_m J_n(\xi_m r) \tag{9a}$$

$$S_{II}(r) = \sum_{m=1}^{\infty} T_m \rho_m J_n(\rho_m r) \tag{9b}$$

$$S_z(r) = \sum_{m=1}^{\infty} Z_m J_n(\xi_m r), \tag{9c}$$

where

$$U_{\mathrm{I}} = \frac{1}{r}\frac{\mathrm{d}}{\mathrm{d}r}(rU_r) + \frac{n}{r}U_\theta$$

$$U_{\mathrm{II}} = \frac{1}{r}\frac{\mathrm{d}}{\mathrm{d}r}(rU_\theta) + \frac{n}{r}U_r$$

$$S_{\mathrm{I}} = \frac{1}{r}\frac{\mathrm{d}}{\mathrm{d}r}(rS_r) + \frac{n}{r}S_\theta$$

$$S_{\mathrm{II}} = \frac{1}{r}\frac{\mathrm{d}}{\mathrm{d}r}(rS_\theta) + \frac{n}{r}S_r.$$

Based on the expansions (8) and (9), one can construct the end stiffness matrix [**K**] for the cylinder with the surface condition (5) (which will be called the mixed cylinder from now on):

$$\begin{Bmatrix} \mathbf{Z} \\ \mathbf{S} \\ \mathbf{T} \end{Bmatrix} = [\mathbf{K}] \begin{Bmatrix} \mathbf{W} \\ \mathbf{U} \\ \mathbf{V} \end{Bmatrix} = \begin{bmatrix} \mathbf{K11} & \mathbf{K12} & \mathbf{K13} \\ \mathbf{K21} & \mathbf{K22} & \mathbf{K23} \\ \mathbf{K31} & \mathbf{K32} & \mathbf{K33} \end{bmatrix} \begin{Bmatrix} \mathbf{W} \\ \mathbf{U} \\ \mathbf{V} \end{Bmatrix} \tag{10}$$

with

$$\mathbf{Z} = \begin{Bmatrix} Z_1 \\ Z_2 \\ \cdots \\ Z_{n_h} \end{Bmatrix}; \quad \mathbf{S} = \begin{Bmatrix} S_1 \\ S_2 \\ \cdots \\ S_{n_h} \end{Bmatrix}; \quad \mathbf{T} = \begin{Bmatrix} T_1 \\ T_2 \\ \cdots \\ T_{n_h} \end{Bmatrix}$$

$$\mathbf{W} = \begin{Bmatrix} W_1 \\ W_2 \\ \cdots \\ W_{n_h} \end{Bmatrix}; \quad \mathbf{U} = \begin{Bmatrix} U_1 \\ U_2 \\ \cdots \\ U_{n_h} \end{Bmatrix}; \quad \mathbf{V} = \begin{Bmatrix} V_1 \\ V_2 \\ \cdots \\ V_{n_h} \end{Bmatrix} \tag{11}$$

where n_h is the number of terms in the truncated series expansions of (8) and (9). For general nonsymmetric wave propagation, it is crucial to use the stiffness matrix that relates the modified quantities U_I, U_{II}, S_I and S_{II} as well as the normal components of the displacement and stress; the submatrices of [**K**] are merely diagonal. If one tried to construct a stiffness matrix which relates usual displacement and stress for the nonsymmetric case, the stiffness matrix would not be diagonal.

From the solutions of the mixed cylinder (see Kim and Steele, 1989b), the explicit expressions for the diagonal elements of the stiffness matrix, which are the only nonzero elements in [**K**], can be given as

$$\begin{aligned}
\Delta_j(\mathbf{K11})_{j,j} &= \frac{\Omega^2}{2}(\mathrm{i}\lambda_{sj}) \\
\Delta_j(\mathbf{K12})_{j,j} &= [(\mathrm{i}\lambda_{dj})(\mathrm{i}\lambda_{sj}) - \xi_j^2 + \Omega^2]\xi_j \\
\mathbf{K21}_{j,j} &= \mathbf{K12}_{j,j} \\
\Delta_j(\mathbf{K22})_{j,j} &= \frac{\Omega^2}{2}(\mathrm{i}\lambda_{sj}) \\
\mathbf{K33}_{j,j} &= \mathrm{i}\lambda_{tj} \\
\mathbf{K13} = \mathbf{K23} &= \mathbf{K31} = \mathbf{K32} = 0
\end{aligned} \tag{12}$$

where

$$\Delta_j = \xi_j^2 - (\mathrm{i}\lambda_{dj})(\mathrm{i}\lambda_{sj}); \quad \lambda_{dj}^2 = \alpha^2\Omega^2 - \xi_j^2; \quad \lambda_{sj}^2 = \Omega^2 - \xi_j^2; \quad \lambda_{tj}^2 = \Omega^2 - \rho_j^2. \tag{13}$$

The asymptotic form of [**K**] can be easily obtained.

3. SOLUTION PROCEDURE: MIXED END CONDITIONS

As the first step for developing the solution approach for pure end conditions in the traction-free cylinder, we consider the solution procedure for mixed end conditions, namely, when either (σ_{zz}, u_r, u_θ) or (u_z, σ_{rz}, $\sigma_{\theta z}$) is prescribed at the end of the traction-free cylinder. In the present work, we expand the end displacement and stress quantities of the traction-free cylinder in terms of expansions (8–9). Then, we form the end stiffness matrix of the traction-free cylinder, which relates the expansion coefficients of [$U_z(r)$, $U_I(r)$, $U_{II}(r)$], and [$S_z(r)$, $S_I(r)$, $S_{II}(r)$].

For the mixed end conditions, matrices [**A**] and [**B**] are constructed, which are defined by

$$\begin{Bmatrix} \mathbf{W} \\ \mathbf{S} \\ \mathbf{T} \end{Bmatrix} = [\mathbf{A}] \begin{Bmatrix} \mathbf{Z} \\ \mathbf{U} \\ \mathbf{V} \end{Bmatrix} = \begin{bmatrix} \mathbf{A11} & \mathbf{A12} & \mathbf{A13} \\ \mathbf{A21} & \mathbf{A22} & \mathbf{A23} \\ \mathbf{A31} & \mathbf{A32} & \mathbf{A33} \end{bmatrix} \begin{Bmatrix} \mathbf{Z} \\ \mathbf{U} \\ \mathbf{V} \end{Bmatrix} \tag{14}$$

$$\begin{Bmatrix} \mathbf{Z} \\ \mathbf{U} \\ \mathbf{V} \end{Bmatrix} = [\mathbf{B}] \begin{Bmatrix} \mathbf{W} \\ \mathbf{S} \\ \mathbf{S} \end{Bmatrix} = \begin{bmatrix} \mathbf{B11} & \mathbf{B12} & \mathbf{B13} \\ \mathbf{B21} & \mathbf{B22} & \mathbf{B23} \\ \mathbf{B31} & \mathbf{B32} & \mathbf{B33} \end{bmatrix} \begin{Bmatrix} \mathbf{W} \\ \mathbf{S} \\ \mathbf{T} \end{Bmatrix} \tag{15}$$

where **Z**, **S**, **T**, **W**, **U** and **V** are defined in (11). Obviously [**B**] is simply the inverse of [**A**]; we will directly compute either one depending on the end conditions.

In order to construct [**A**] and [**B**], we first expand the components of the eigenfunctions of the traction-free cylinder as:

$$\tilde{u}_z^p(r) = \sum_{m=1}^{n_h} W_m^p J_n(\xi_m r) \tag{16a}$$

$$\tilde{u}_I^p(r) = \sum_{m=1}^{n_h} \xi_m U_m^p J_n(\xi_m r) \tag{16b}$$

$$\tilde{u}_{II}^p(r) = \sum_{m=1}^{n_h} \rho_m V_m^p J_n(\rho_m r) \tag{16c}$$

$$\tilde{\sigma}_{zz}^p(r) = \sum_{m=1}^{n_h} Z_m^p J_n(\xi_m r) \tag{16d}$$

$$\tilde{\sigma}_I^p(r) = \sum_{m=1}^{n_h} \xi_m S_m^p J_n(\xi_m r) \tag{16e}$$

$$\tilde{\sigma}_{II}^p(r) = \sum_{m=1}^{n_h} \rho_m T_m^p J_n(\rho_m r). \tag{16f}$$

One can show that the coefficients W_m^p, etc. in (16) can be determined in closed form. Note that no contribution comes from $\tilde{\sigma}_{rz}^p(r)|_{r=1}$ for S_m^p, but that $\tilde{u}_r^p(r)|_{r=1}$ does contribute to U_m^p. [$\tilde{\sigma}_{rz}^p(r)|_{r=1} = 0$, and $u_r^p(r)|_{r=1} \neq 0$.] Therefore, we have

$$U_I^p = \hat{U}_I^p - \frac{\eta_m}{\xi_m} J_n(\xi_m) \tilde{u}_r^p(r)|_{r=1}$$

where $\hat{U}_I^p$ denotes the quantity obtained by assuming $\tilde{u}_r(r)|_{r=1} = 0$.

We consider the following end conditions in order to form the elements of the matrix [**A**]. First, consider an end condition at $z = 0$ such that

$$\begin{cases} S_z(r) = J_n(\xi_m r) \\ U_I(r) = 0 \\ U_{II}(r) = 0 \end{cases} \tag{17}$$

for a given frequency Ω. The pth expansion coefficient E_m^p for the end condition (17) can be obtained using the bi-orthogonality as

$$E_m^p = \frac{1}{D^p} \int_0^1 J_n(\xi_m r) \tilde{u}_z^p(r) r \, dr = \frac{1}{D^p} \eta_m W_m^p$$

where D^p is defined in (4) and η_m is defined as $2\xi_m^2/(\xi_m^2 - n^2) J_n^2(\xi_m)$.

Then the corresponding normal displacement $[U_z(r)]_m$ at $z = 0$ can be expressed as

$$\begin{aligned} [U_z(r)]_m &= \sum_{p=1}^{n_e} E_m^p \tilde{u}_z^p(r) \\ &= \sum_{p=1}^{n_e} \sum_{l=1}^{n_h} E_m^p W_l^p J_n(\xi_m r) \\ &= \sum_{l=1}^{n_h} J_n(\xi_m r) \left[\sum_{p=1}^{n_e} E_m^p W_l^p \right] \end{aligned} \tag{18}$$

where n_e denotes the number of eigenfunctions used for the traction-free cylinder. Similarly, the two modified stress quantities can be calculated:

$$[S_I(r)]_m = \sum_{l=1}^{n_h} J_n(\xi_m r) \left[\sum_{p=1}^{n_e} E_m^p S_m^p \right] \tag{19}$$

$$[S_{II}(r)]_m = \sum_{l=1}^{n_h} J_n(\rho_m r) \left[\sum_{p=1}^{n_e} E_m^p T_m^p \right]. \tag{20}$$

Thus the components of **A11**, **A21**, and **A31** are expressed as

$$(\mathbf{A11})_{l,m} = \sum_{p=1}^{n_e} E_m^p W_l^p \quad \text{for} \quad l = 1, 2, \ldots, n_h \tag{21a}$$

$$(\mathbf{A21})_{l,m} = \sum_{p=1}^{n_e} E_m^p S_l^p \quad \text{for} \quad l = 1, 2, \ldots, n_h \tag{21b}$$

$$(\mathbf{A31})_{l,m} = \sum_{p=1}^{n_e} E_m^p T_l^p \quad \text{for} \quad l = 1, 2, \ldots, n_h \tag{21c}$$

for $m = 1, 2, \ldots, n_h$.

By considering the end condition such that

$$\begin{cases} S_z(r) = 0 \\ U_I(r) = \xi_m J_n(\xi_m r) \\ U_{II}(r) = 0 \end{cases} \tag{22}$$

the elements of **A12**, **A22**, and **A32** can be evaluated. The actual end condition corresponding to (22) in terms of $U_r(r)$ and $U_\theta(r)$ is

$$\begin{cases} S_z(r) = 0 \\ U_r(r) = -\dfrac{1}{\xi_m} \dfrac{\mathrm{d}J_n(\xi_m r)}{\mathrm{d}r} \\ U_\theta(r) = \dfrac{1}{\xi_m} \dfrac{n}{r} J_n(\xi_m r). \end{cases}$$

Following the same steps for **A11**, **A21** and **A31**, the components of **A12**, etc. can be computed.

Similarly, closed-form expressions for the elements of other submatrices of [**A**] and [**B**] can be obtained. For later use, F_m^p, G_m^p, H_m^p, H_m^p, I_m^p and J_m^p are used to designate the expansion coefficients for the end conditions

$$[S_z(r) = 0, \quad U_I(r) = \xi_m J_n(\xi_m r), \quad U_{II}(r) = 0],$$

$$[S_z(r) = 0, \quad U_I(r) = 0, \quad U_{II}(r) = \rho_m J_n(\rho_m r)],$$

$$[U_z(r) = J_n(\xi_m r), \quad S_I(r) = 0, \quad U_{II}(r) = 0],$$

$$[U_z(r) = 0, \quad S_I(r) = \xi_m J_n(\xi_m r), \quad U_{II}(r) = 0]$$

and

$$[U_z(r) = 0, \quad S_I(r) = 0, \quad U_{II}(r) = \rho_m J_n(\rho_m r)],$$

respectively.

For mixed end conditions which have been discussed in this section, the bi-orthogonality property [see eqn (4)] can be directly used. However, the matrices [**A**] and [**B**] will be required in forming the stiffness and flexibility matrices for pure end problems.

4. SOLUTION PROCEDURE: PURE END CONDITIONS

When either $(\sigma_{zz}, \sigma_{rz}, \sigma_{\theta z})$ or (u_z, u_r, u_θ) is specified at the end of the cylinder, the bi-orthogonality property is not directly applicable. The purpose of the present work is to develop an efficient solution procedure which is applicable for pure end problems and useful for both rapidly and slowly varying end conditions.

The present approach uses the following end stiffness matrix [**S**] (which is useful for

displacement end conditions):

$$\begin{Bmatrix} \mathbf{Z} \\ \mathbf{S} \\ \mathbf{T} \end{Bmatrix} = [\mathbf{S}] \begin{Bmatrix} \mathbf{W} \\ \mathbf{U} \\ \mathbf{V} \end{Bmatrix} = \begin{bmatrix} \mathbf{S11} & \mathbf{S12} & \mathbf{S13} \\ \mathbf{S21} & \mathbf{S22} & \mathbf{S23} \\ \mathbf{S31} & \mathbf{S32} & \mathbf{S33} \end{bmatrix} \begin{Bmatrix} \mathbf{W} \\ \mathbf{U} \\ \mathbf{V} \end{Bmatrix}. \tag{23}$$

The submatrices of [S] can be determined from the matrix [A] in (14) as

$$\begin{aligned} &\mathbf{S11} = \mathbf{A11}^{-1} \quad \mathbf{S12} = -\mathbf{S11} \cdot \mathbf{A12} \quad \mathbf{S13} = -\mathbf{S11} \cdot \mathbf{A13} \\ &\mathbf{S21} = \mathbf{A21} \cdot \mathbf{S11} \quad \mathbf{S22} = \mathbf{A22} + \mathbf{A21} \cdot \mathbf{S12} \quad \mathbf{S23} = \mathbf{A23} + \mathbf{A21} \cdot \mathbf{S13} \\ &\mathbf{S31} = \mathbf{A31} \cdot \mathbf{S11} \quad \mathbf{S32} = \mathbf{A32} + \mathbf{A31} \cdot \mathbf{S12} \quad \mathbf{S33} = \mathbf{A33} + \mathbf{A31} \cdot \mathbf{S13}. \end{aligned} \tag{24}$$

Following the procedure used to determine the stiffness matrix [S], the flexibility matrix [F] for stress end conditions can be also constructed such that

$$\begin{Bmatrix} \mathbf{Z} \\ \mathbf{S} \\ \mathbf{T} \end{Bmatrix} = [\mathbf{F}] \begin{Bmatrix} \mathbf{W} \\ \mathbf{U} \\ \mathbf{V} \end{Bmatrix} = \begin{bmatrix} \mathbf{F11} & \mathbf{F12} & \mathbf{F13} \\ \mathbf{F21} & \mathbf{F22} & \mathbf{F23} \\ \mathbf{F31} & \mathbf{F32} & \mathbf{F33} \end{bmatrix} \begin{Bmatrix} \mathbf{W} \\ \mathbf{U} \\ \mathbf{V} \end{Bmatrix}. \tag{25}$$

Replacing [A] and [S] by [B] and [F], respectively, in (24) gives the expression for the submatrices of [F].

Since the end stiffness (or flexibility) matrix relates the displacement and stress quantities only at the end, a procedure to compute the stress/displacement at z other than 0 from the end stiffness (or flexibility) matrix is necessary. To this end, the expansion coefficients in (3) should be determined. The procedure to compute E^p is as follows.

If $[U_z(r) \neq 0, U_I(r) = U_{II}(r) = 0]$ is prescribed where $U_z(r)$ is given by (8c), we compute $S_z(r)$ from the present end stiffness, and then regard the end condition as a mixed end condition $[S_z(r) \neq 0, U_I(r) = U_{II}(r) = 0]$. For this mixed end condition, we obtain

$$E^p = \sum_{m=1}^{n_h} E_m^p \left[\sum_{l=1}^{n_h} (\mathbf{S11})_{m,l} W_l \right]. \tag{26}$$

If $[U_z(r) = 0, U_I(r) \neq 0, U_{II}(r) = 0]$ is given with the expansion (8a) for $U_1(r)$, $S_z(r)$ is first computed by means of the stiffness matrix and the end condition is assumed to be $[S_z(r) \neq 0, U_I(r) \neq 0, U_{II}(r) = 0]$.† Then the expansion coefficient E^p may be written as

$$E^p = \sum_{m=1}^{n_h} E_m^p \left[\sum_{l=1}^{n_h} (\mathbf{S12})_{m,l} U_l \right] + \sum_{m=1}^{n_h} F_m^p U_m. \tag{27}$$

Similarly for $[U_z(r) = 0, U_I(r) = 0, U_{II}(r) \neq 0]$ in which $U_{II}(r)$ is expressed by (8b), E^p is given by

$$E^p = \sum_{m=1}^{n_h} E_m^p \left[\sum_{l=1}^{n_h} (\mathbf{S13})_{m,l} V_l \right] + \sum_{m=1}^{n_h} G_m^p V_m. \tag{28}$$

The expansion coefficients for general displacement end conditions can be obtained by superposition of the results (26), (27) and (28). The same step can be followed for stress end conditions.

5. ASYMPTOTIC BEHAVIOR OF THE STIFFNESS MATRIX

The stiffness matrix for $n = 2$, $\nu = 0.3317$ and $\Omega = 2.0$‡ has been computed and its asymptotic nature is investigated. We choose $n_h = 40$ ($n_e = 240$) to construct the stiffness matrix.

† Or we can compute $S_I(r)$ and $S_{II}(r)$ first, and replace the pure end condition by the mixed end condition $[U_z(r) = 0, S_I(r) \neq 0, S_{II}(r) \neq 0]$, but there is no advantage; in fact, less accurate results for E^p were obtained.

‡ For the present choice of Ω, [S] and [K] are real-valued.

In Fig. 1, the diagonal elements of the submatrices of [S] are compared with those of [K]. Figure 1a shows the relative differences of $\mathbf{SII}_{j,j}$ with respect to $\mathbf{KII}_{j,j}$ for **I** = **1**, **2** and **3**, and it is apparent that the diagonal elements of [S] approach those of [K] rapidly. The magnitudes of the diagonal elements of **S13**, **S23**, **S31** and **S32** are also plotted in Fig. 1b. This figure shows that the diagonal elements of **S13**, etc. approach the counterparts of **K13**, etc., which are identically zero. Since the increase rates of the diagonal elements of **S11**, etc. are approximately linear in j (the index number), the relative decrease rates of the diagonal elements of **S13**, etc. with respect to the diagonal elements of **S11**, etc. are very rapid.

The present observation for $\mathbf{SIJ}_{I,J}$ and the investigation of the nature of the diagonal dominance of all submatrices of S suggest the following asymptotic form of the stiffness matrix (see Kim, 1989b for more details):

$$\mathbf{SIJ} = \begin{bmatrix} \mathbf{SIJU} & \mathbf{SIJR} \\ \mathbf{SIJL} & \mathbf{SIJD} \end{bmatrix}$$

$$\mathbf{SIJD} \approx \mathbf{KIJ} \qquad \text{for } \mathbf{I}, \mathbf{J} = \mathbf{1}, \mathbf{2} \text{ or } \mathbf{3}. \tag{29}$$

This structure (29) also applies to [A], [B] and [F].

The advantages of using the asymptotic structure (29) are clear. First, **SIJD** is simply replaced by **KIJ** which are easily computed. Secondly, the matrix inversion of the form (29) requires only the inversion of **SIJU** ([S] represents any of [S], [F], [A] and [B]) so that this form is very useful for end problems requiring very many spatial harmonics. For detailed accounts of this, refer to Kim and Steele (1989a). As in the axisymmetric case, we denote the array size of **SIJU** by n_u. For other values of n, ν and Ω, similar asymptotic behavior of the stiffness matrix was observed.

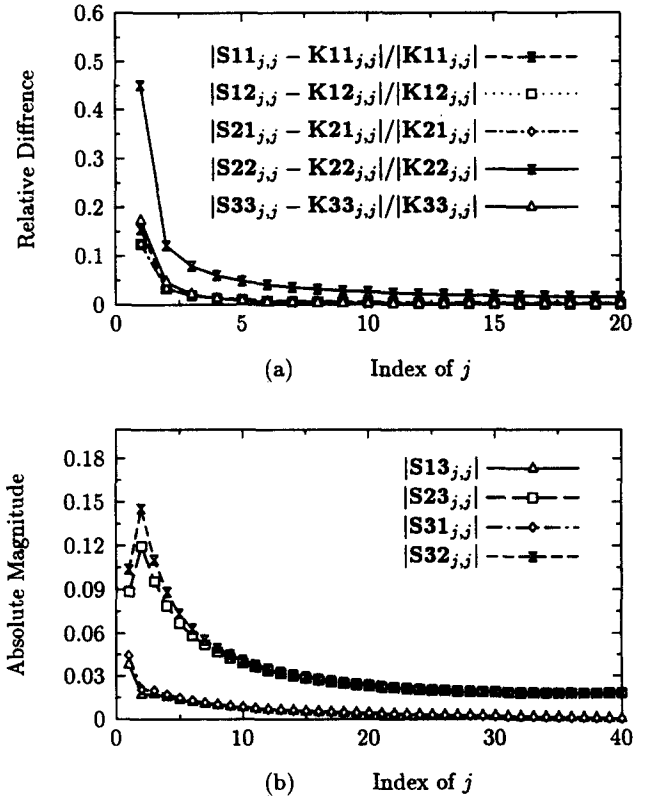

Fig. 1. Comparison of the diagonal elements of the end stiffness matrix [S] of the traction-free cylinder with those of the end stiffness matrix [K] of the mixed cylinder (n = 2, ν = 0.3317, Ω = 2). It is seen that [S] asymptotically approaches [K].

6. NUMERICAL EXAMPLES

Case 1

The first numerical example deals with a nonzero $U_{II}(r)$ end condition [$U_z(r) = U_t(r) = 0$] such that ($n = 2$, $\nu = 0.3317$, $\Omega = 2$)†

$$\begin{cases} U_z(r) = 0 \\ U_r(r) = \sin 3\pi r \\ U_\theta(r) = -(\sin 3\pi r + 3\pi r \cos 3\pi r)/n. \end{cases} \tag{30}$$

Figure 2 shows the stress distributions at $z = 0$ for the end condition (30) by the present method with ($n_h = 40$, $n_u = 20$, $n_e = 240$) and the collocation method with $n_e = 600$. The present results pass through the averages of the results obtained by collocation, which exhibit local oscillatory behavior. The local oscillations appearing in the results by the collocation methods must be due to the slow convergence for higher modes.

The first few expansion coefficients E^p in (3) are listed in Table 1 for different numbers of unknowns. As Table 1 shows, both the present and collocation methods appear to converge rapidly for this relatively slowly varying end condition. Note that almost identical results for the first few expansion coefficients are obtained regardless of the use of the structure (29).

The components of the displacement and stress at various values of z ($z = 0.5$, 1, 10 and 20) have been also computed and good agreement was observed. Tables 2 and 3 show the CPU times in obtaining the solutions at the several values of z, and substantial saving in the CPU time by the present method is apparent.

Case 2

Consider the following patch loading condition at $z = 0$ such that

$$\begin{cases} \sigma_{zz}|_{z=0} = \begin{cases} 1 \text{ for } 3/8 < r < 5/8 \text{ and } -\pi/8 < \theta < \pi/8 \\ 0 \text{ elsewhere} \end{cases} \\ \sigma_{rz} = \sigma_{\theta z} = 0. \end{cases}$$

The solution for this nonsymmetric loading case has been obtained by the present approach with $n_f = 20$, $n_h = 40$ and $n_u = 20$, where n_f denotes the highest term in the Fourier series in the circumferential direction.‡

Table 1. Expansion coefficients for Case 1

$\lvert E^p \rvert$	$\lvert E^1 \rvert = \lvert E^2 \rvert$	$\lvert E^3 \rvert$	$\lvert E^4 \rvert = \lvert E^5 \rvert$
Collocation $n_e = 150$	0.2765E0	0.2160E0	0.2607E−1
Collocation $n_e = 300$	0.2805E0	0.2166E0	0.2629E−1
Collocation $n_e = 600$	0.2817E0	0.2168E0	0.2635E−1
Present $n_h = n_u = 20$, $n_e = 120$	0.2860E0	0.2175E0	0.2657E−1
Present $n_h = 40$, $n_u = 20$, $n_e = 240$	0.2841E0	0.2171E0	0.2645E−1
Present $n_h = n_u = 40$, $n_e = 240$	0.2838E0	0.2171E0	0.2646E−1

† More numerical examples obtained by the present approach can be found in Kim (1989b).

‡ The contribution of the $n = 0$ mode has been taken into account by the method by Kim and Steele (1989a).

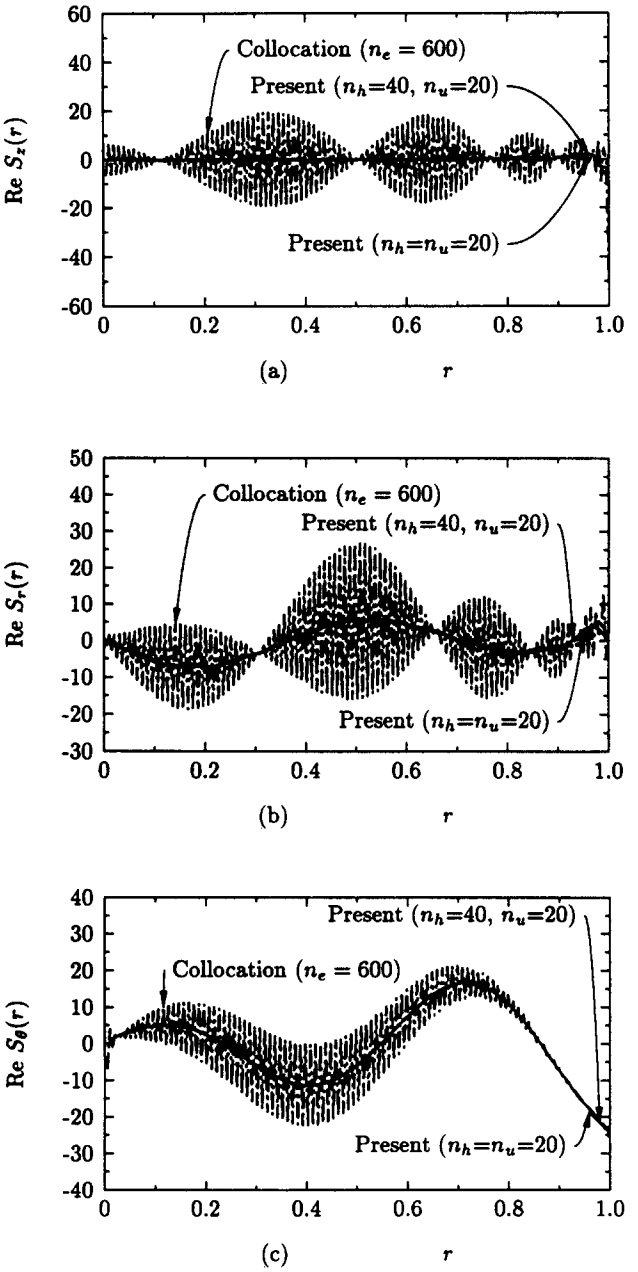

Fig. 2. Stress distributions at $z = 0$ due to the end condition $[U_z(r) = 0,\ U_r(r) = \sin 3\pi r,\ U_\theta(r) = -(\sin 3\pi r + 3\pi r \cos 3\pi r)/n]$ for $n = 2$, $\nu = 0.3317$, $\Omega = 2$. (a) $\mathscr{R}[S_z(r)]$, (b) $\mathscr{R}[S_r(r)]$, and (c) $\mathscr{R}[S_\theta(r)]$.

Table 2. CPU time by collocation for Case 1 on Convex C-1

$n_c = 150$	$n_c = 300$	$n_c = 600$
312 s	1201 s	5745 s

Figure 3 shows the real part of the deformed configuration of the end surface of the cylinder (at $z = 0$) and the contour of the absolute value of $\mathscr{R}[\sigma_{zz}|_{z=0}]$. The undeformed configuration of the end surface is shown by the black mesh. It is seen that the real part of the normal stress is reasonably well approximated with the present number of n_f and n_h. Note that the real part of the end displacement is associated with end effects and the imaginary part of the end displacement (though not shown here) corresponds to energy propagation.

Figures 4, 5 and 6 show the absolute values of $\mathscr{R}[\sigma_{zz}]$ plotted on the real parts of the deformed configurations of the cross-sections of the cylinder at $z = 0.5$, 1 and 10, respectively. At $z = 0.5$, the localized distribution of $\mathscr{R}[\sigma_{zz}]$ is still noticeable, but at $z = 1$, the localized effect of the patch load applied at $z = 0$ has almost disappeared. The rapidly attenuating nature of the end effect is well demonstrated in Figs 4, 5 and 6.

The imaginary part of σ_{zz} at $z = 1$ is also plotted on the imaginary part of the deformed configuration in Fig. 7. The stress distribution is almost linear in x $(= r \cos \theta)$, which appears reasonable. Other stress components were computed by the present method, and the convergence of the present solutions was confirmed by considering solutions with different numbers of terms in the series expansions in θ and r.

7. CONCLUSIONS

An analytic–asymptotic solution approach has been proposed for time-harmonic non-symmetric wave propagation in a cylinder. The present solution procedure for general end conditions employs the end stiffness matrix, which relates not only the normal components of the displacement and stress but also the modified displacement and stress quantities introduced by Kim and Steele (1989b). The use of such a stiffness matrix is crucial because asymptotic solutions can be easily incorporated this way.

Numerical examples indicate that the present method is much more efficient than conventional solution techniques such as collocation in handling general end conditions and is capable of capturing accurately both the solution parts corresponding to local end effects and to the far field.

Table 3. CPU time by present approach for Case 1 on Convex C-1

$n_h = n_u = 20$	$n_h = n_u = 40$	$n_h = 40$, $h_u = 20$
62 s	181 s	117 s

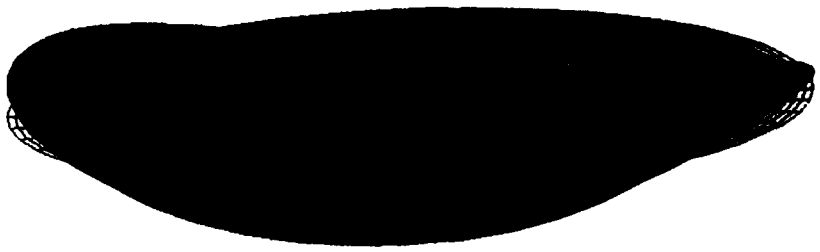

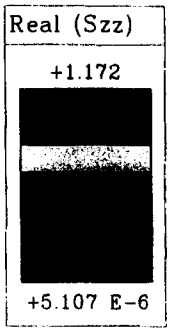

Fig. 3. Recalculated normal stress at the end surface of the cylinder (at $z = 0$) on the real part of the deformed configuration for Case 2 (Patch Loading). The localized normal displacement can be seen ($\Omega = 2, \nu = 0.3317$). The black mesh represents the undeformed configuration.

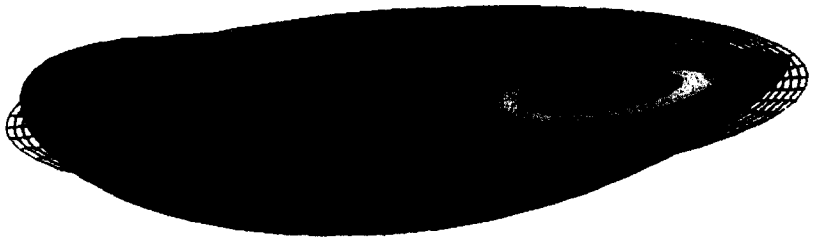

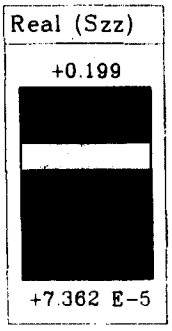

Fig. 4. $\mathscr{R}[\sigma_{zz}]$ on the real part of the deformed configuration at $z = 0.5$. The stress concentration for $\mathscr{R}[\sigma_{zz}]$ is still noticeable.

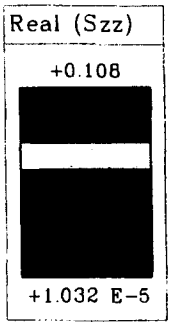

Fig. 5. $\mathscr{R}[\sigma_{zz}]$ on the real part of the deformed configuration at $z = 1$. The real part of the normal stress appears to be no longer localized.

Fig. 6. $\mathscr{R}[\sigma_{zz}]$ on the real part of the deformed configuration at $z = 10$.

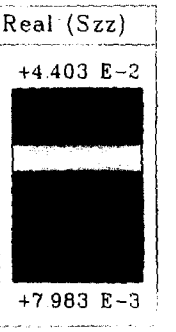

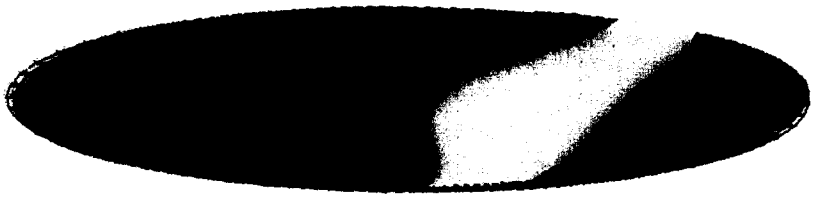

Fig. 7. $\mathscr{I}[\sigma_{zz}]$ on the imaginary part of the deformed configuration at $z = 1$. The stress distribution is almost linear in $x = r\cos\theta$ as expected.

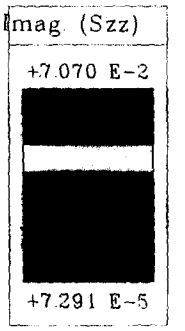

Acknowledgements—This work was partially supported by Grant MSM-8814355 from the National Science Foundation. The authors are grateful to Juan Simo and Steven Rifai for the use of their graphic package in the preparation of the figures. We also thank the reviewers for their comments on the earlier version of the manuscript.

REFERENCES

Devault, G. P. and Curtis, C. W. (1962). Elastic cylinder with free lateral surface and mixed time-dependent end conditions. *J. Acoust. Soc. Am.* **34,** 421–432.

Frazer, W. B. (1975). An orthogonality relation for the modes of wave propagation in an elastic circular cylinder. *J. Sound Vibr.* **43,** 568–571.

Green, W. A. (1960). Dispersion relations for elastic waves in bars. In *Progress in Solid Mechanics* (Edited by I. N. Sneddon and R. Hill), pp. 223–261. North Holland, Amsterdam.

Gregory, R. D. (1983). A note on bi-orthogonality relations for elastic cylinders of general cross section. *J. Elasticity* **13,** 351–355.

Kim, Y. Y. (1989a). Uncoupled wave systems and dispersion in an infinite solid cylinder. *J. Appl. Mech.* **56,** 347–355.

Kim, Y. Y. (1989b). End effects and time-harmonic wave propagation in a semi-infinite solid cylinder. Ph.D. Thesis, Stanford University, Stanford, California.

Kim, Y. Y. and Steele, C. R. (1989a). End effects and time-harmonic longitudinal wave propagation in a semi-infinite solid cylinder. *J. Appl. Mech.* **56,** 334–346.

Kim, Y. Y. and Steele, C. R. (1989b). Effects of lateral surface conditions in time-harmonic nonsymmetric wave propagation in a cylinder. *J. Appl. Mech.* **56,** 910–917.

McKenna, J. and Simplins, P. G. (1985). Model solutions, symmetry properties, and orthogonality conditions for elastic waves in cylinders. *J. Acoust. Soc. Am.* **78,** 1675–1683.

McNiven, H. D. and McCoy, J. J. (1974). Vibrations and wave propagation in rods. In *R. D. Mindlin and Applied Mechanics* (Edited by G. Herrmann), pp. 197–226. Pergamon Press, New York.

Miklowitz, J. (1966). Elastic wave propagation. In *Applied Mechanics Survey* (Edited by H. N. Abramson, H. Liebowitz, J. N Crowley and S. Juhasz), pp. 809–839. Spartan Books, Washington.

Pao, Y.-H. (1983). Elastic waves in solids. *J. Appl. Mech.* **50,** 1152–1164.

Shen, S.-Q. (1988). Transient elastic waves in a circular cylinder. Ph.D. Thesis, Cornell University, Ithaca, New York.

Wilson, L. O. (1986). The response of a semi-infinite fiber to a pulse applied asymmetrically to its end. *J. Acoust. Soc. Am.* **79,** 1798–1810.

Zemanek, J. (1972). An experimental and theoretical investigation of elastic wave propagation in a cylinder. *J. Acoust. Soc. Am.* **51,** 265–283.